OH–IR STARS. I. PHYSICAL PROPERTIES OF CIRCUMSTELLAR ENVELOPES*

PETER GOLDREICH AND NICK SCOVILLE
California Institute of Technology
Received 1975 June 16

ABSTRACT

A theoretical model of the circumstellar envelope which surrounds a OH–IR star is developed. The circumstellar gas is ejected by radiation pressure which acts on dust grains that condense in the atmosphere of the central star. The dust grains transfer momentum to the gas by collisions with the gas molecules. These collisions are the dominant source of heat input to the circumstellar gas. The major sources of cooling are the emission of radiation by H_2O molecules and adiabatic expansion. The gas temperature decreases from $T \approx 2 \times 10^3$ K near the stellar surface at $r \approx 6 \times 10^{13}$ cm, to $T \approx 8 \times 10^2$ K at $r = 10^{15}$ cm and to $T \approx 10^2$ K at $r = 10^{16}$ cm. The OH molecule abundance in the circumstellar envelope is controlled by chemical exchange reactions and by the dissociation of H_2O molecules. The reaction $OH + H_2 \leftrightarrow H_2O + H + 0.69$ eV, which has an activation energy of 0.3 eV, rapidly converts OH molecules into H_2O molecules in the warm ($T \gtrsim 5 \times 10^2$ K) inner ($r \lesssim 2 \times 10^{15}$ cm) region of the circumstellar envelope. Beyond $r \approx 2 \times 10^{15}$ cm, T is so low that the exchange reaction is very slow and the mean lifetime of an OH molecule is greater than the expansion time scale for the circumstellar envelope. In the outer region of the circumstellar envelope, OH molecules are produced from the photodissociation of H_2O molecules by the interstellar ultraviolet radiation and from the dissociation of H_2O molecules by collisions with dust grains. These processes are capable of producing OH number densities greater than 1 cm^{-3} at $r \approx 10^{16}$ cm.

The predicted values of the gas temperature, T, and the OH abundance, n_{OH}, depend upon the rate of mass loss from the central star, Φ. The results quoted above are based on a calculation with $\Phi = 3 \times 10^{-5} M_\odot$ yr^{-1}. In general, T varies inversely and n_{OH} varies directly with Φ.

Subject headings: infrared: sources — stars: circumstellar shells

I. INTRODUCTION

It is known that OH and H_2O masers operate in circumstellar envelopes about late M-type Mira variables and supergiants. These are cool ($T_e \approx 2 \times 10^3$ K), high luminosity ($L \approx 10^4 L_\odot$), oxygen rich ([O]/[C] > 1), evolved stars. It is necessary to determine the physical conditions in the circumstellar envelopes as a prerequisite for detailed modeling of the maser pump mechanisms. Unfortunately, observations of the gaseous components of the circumstellar envelopes are very limited. In particular, the gas kinetic temperature and the OH and H_2O abundances are not observationally determined. The principal goal of this investigation is to theoretically determine these quantities. The plan of the paper is as follows. Section II is devoted to developing the basic equations which describe the evolution of v, T, n_{OH}, and n_{H_2O} in the circumstellar gas. These equations are numerically integrated and the results obtained are discussed in § III. In § IV consideration is given to the production of OH molecules due to the photodissociation of H_2O molecules by the interstellar ultraviolet radiation. The production of OH molecules due to the collisional dissociation of H_2O molecules by dust grains is described in § V. Finally, § VI contains an estimate

of the variation in T that is driven by a periodic luminosity variation of the central star.

II. CIRCUMSTELLAR ENVELOPE

In the interest of simplicity, a definite model is adopted for all numerical calculations. For future reference, numerical values for all of the relevant parameters are listed here. They are as follows: stellar mass $M = 1 M_\odot = 2 \times 10^{33}$ gm; stellar luminosity $L = 10^4 L_\odot = 4 \times 10^{37}$ ergs s^{-1}; stellar radius $R = 6 \times 10^{13}$ cm; stellar effective temperature $T_e = 2 \times 10^3$ K; mass loss rate $\Phi = 3 \times 10^{-5} M_\odot$ yr^{-1}; terminal velocity of circumstellar gas $v_\infty = 20$ km s^{-1}; ratio of atomic to molecular hydrogen by number in the circumstellar gas $n_H/n_{H_2} = 1$; ratios of total numbers of C, O, and H nuclei in the circumstellar gas [C]/[H] = 3×10^{-4}, [O]/[H] = 8×10^{-4}. These numbers should be borne in mind during the reading of the section, although the equations developed here do not make explicit use of them.

a) Dynamics

The acceleration of gas away from the central stars in OH–IR sources is believed to be due to radiation pressure acting on dust grains which form in the escaping gas (Salpeter 1974; Kwok 1975). It is also possible that the gas receives at least part of its initial

144

acceleration from shock waves which propagate out from the stellar atmospheres. However, only acceleration by radiation pressure is considered in this paper.

Beyond the sonic point, thermal pressure is unimportant and the equation of motion for the ejected gas takes the form

$$v \frac{dv}{dr} = \frac{\kappa(r)L}{4\Pi r^2 c} - \frac{GM}{r^2} \cdot \quad (1)$$

Here r is the radial distance from the center of the star, $\kappa(r)$ is the dust opacity per unit mass

$$\kappa(r) = \frac{Q n_d \sigma_d}{m_{H_2} n_{H_2}(1 + f/2)}, \quad (2)$$

where n_d, σ_d, and Q are, respectively, the number density, the geometrical cross section, and the momentum transfer efficiency factor of the dust grains, and $f = n_H/n_{H_2}$. In writing equation (1), it has been implicitly assumed that the mass outflow is steady in time and that the circumstellar dust is optically thin to the stellar radiation. The latter assumption is a marginal one for a few of the most highly reddened OH–IR stars.

The radial dependence of $\kappa(r)$ is not well determined observationally. Infrared measurements of one Mira variable, IRC +10011, during a lunar occultation (Zappala *et al.* 1974) indicate that $\kappa(r)$ probably increases from stellar surface to about $r = 10 R$. On the other hand, theoretical considerations suggest that most of the refractory material should condense into dust grains within a few stellar radii. The observational indications are heeded here, and $\kappa(r)$ is taken to be of the form

$$\kappa(r) = \Gamma \left(1 + \frac{\Delta r^2}{[(10 R)^2 + r^2]}\right) \cdot \quad (3)$$

In numerical applications Γ and Δ are chosen such that $dv/dr = 0$ at $r = R$ and $v_\infty = 20$ km s^{-1}. For the standard values, $\Phi = 3 \times 10^{-5} M_\odot$ yr^{-1}, and $R = 6 \times 10^{13}$ cm, $\Gamma = 1.18$ cm^2 gm^{-1}, and $\Delta = 7$.

b) Gas Kinetic Temperature

The first law of thermodynamics applied to the escaping gas reads

$$\frac{du}{dt} = \frac{P}{\rho^2} \frac{d\rho}{dt} - \frac{dq}{dt}, \quad (4)$$

where u is the internal energy per unit mass, P is the gas pressure, ρ is the mass density, and q is the net rate of energy loss per unit mass. With the aid of the equation of continuity and the perfect gas law, the work term may be cast in the form

$$\frac{P}{\rho^2} \frac{d\rho}{dt} = \frac{-kT(1 + f)}{m_{H_2}(1 + f/2)} \left(\frac{\partial v}{\partial r} + \frac{2v}{r}\right) \cdot \quad (5)$$

The net rate of heat loss per unit mass may be written

in terms of the total rates of heat input per unit volume H and heat loss per unit volume C as

$$\frac{dq}{dt} = \frac{C - H}{m_{H_2} n_{H_2}(1 + f/2)} \cdot \quad (6)$$

Expressions for H and C are developed in § IIc. The internal energy per unit mass is given by

$$u = \frac{3}{2} \frac{kT(1 + f)}{m_{H_2}(1 + f/2)}, \quad (7)$$

where the H_2 molecules as well as the H atoms are treated as monatomic (i.e., $\gamma = 5/3$ is used for both species). Corrections to γ due to the rotational excitation of the H_2 molecules are significant for $T \gtrsim 300$ K. However, their neglect introduces only minor quantitative errors which are undoubtedly smaller than those due to uncertainties in the expressions for H and C. The equation which governs the radial variation of T is obtained by substituting equations (5)–(7) into equation (4). It reads

$$\frac{1}{T} \frac{dT}{dr} = \frac{-4}{3r} \left(1 + \frac{1}{2} \frac{d \ln v}{d \ln r}\right) + \frac{2(H - C)}{3 v n_{H_2} kT(1 + f)} \cdot \quad (8)$$

c) Heating and Cooling Processes

i) Collisions between Gas Molecules and Dust Grains

The material in the circumstellar envelope is accelerated away from the central star by radiation pressure. The radiation pressure acts directly on the dust grains, and momentum is transferred to the gas by collisions between the gas molecules and the dust grains. These collisions are the dominant source of heat input to the gas. The heat input per unit volume is

$$H \approx \tfrac{1}{2} m_{H_2} n_{H_2}(1 + f/2) v_d^3 \sigma_d n_d, \quad (9)$$

where v_d is drift velocity of the dust grains through the gas:

$$v_d \approx \left(\frac{QL}{4\pi r^2 c m_{H_2} n_{H_2}(1 + f/2)}\right)^{1/2} = \left(\frac{QLv}{\Phi c}\right)^{1/2} \cdot \quad (10)$$

In deriving equations (9) and (10), it has been assumed that v_d is much larger than the sound speed in the gas. This is a good assumption except very close to the stellar atmosphere. In applications of equation (10), the value of $Q = \tfrac{1}{2}$ is always assumed. Substituting the standard parameter values in equation (10) yields $v_d = 9$ km s^{-1}. This value of v_d is significantly below the value, ~ 20 km s^{-1}, at which significant ablation of dust grains by sputtering is believed to occur (Wickramasinghe 1972; Kwok 1975).

ii) Rotational Excitation of H_2O Molecules

At low temperatures ($T \lesssim 10^3$ K), the most important radiative cooling mechanisms involve the collisional excitation of the rotational levels of abundant molecules. Those collisional excitations that are followed by radiative decays in which the emitted

photon escapes from the circumstellar envelope result in a net cooling of the gas. Hydrogen molecules are not significant contributors to this process (except at very low densities, $n_{H_2} \lesssim 10^3 \text{ cm}^{-3}$) because the radiative lifetimes of their excited rotational levels are so long. The H_2O molecule is probably next in abundance to the H_2 molecule in the circumstellar gas. By virtue of its substantial dipole moment (~ 1.94 debye) and large rotational level spacing, the H_2O molecule dominates the radiative cooling of the circumstellar gas at low temperatures.

It is not possible, at present, to accurately calculate the H_2O rotational cooling. Very little is known, from either experiment or theory, about the cross sections for the rotational excitation of H_2O molecules by collisions with H atoms and H_2 molecules. Even if this fundamental data were available, it would still be a formidable task to calculate an accurate cooling law. Such a calculation would have to contend with the fact that many of the H_2O rotational transitions are optically thick in the circumstellar envelope. It would also be necessary to include the excitation of the rotational levels by the stellar radiation field, particularly the indirect excitations due to the absorption of near infrared photons in the fundamental rotation-vibration bands followed by radiative decays back to the ground vibrational state.

Although an accurate calculation of the H_2O rotational cooling is beyond reach, an approximate calculation is carried out in the Appendix. This calculation takes into account the optical depths in both the pure rotation and the rotation-vibration transitions and also includes the excitation of the rotational levels by the stellar radiation. The calculation is based on a classical treatment of the H_2O molecule rotation and the assumption that all of the pure rotational transitions in the ground vibrational state have the same excitation temperature T_x. The result is a relation expressing T_x as a function of L, T_e, T, r, n_H, n_{H_2}, and n_{H_2O}. With T_x and T determined, the H_2O rotational heat loss rate per unit volume may be written as

$$C_1 = n_{H_2}(1 + f)n_{H_2O}\langle\sigma^* v_{\text{th}}\rangle h\nu$$
$$\times\ [\exp(-h\nu/kT) - \exp(-h\nu/kT_x)]\ ,\quad (11)$$

where $\langle\sigma^* v_{\text{th}}\rangle$ is the inelastic collisional rate constant which is set equal to $2 \times 10^{-11}T^{1/2} \text{ cm}^3 \text{ s}^{-1}$ in all numerical applications of equation (11). The frequency ν is the classical value of the rotational frequency of an H_2O molecule whose rotational energy is $3kT_x/2$. Numerically, $\nu(T_x) = 1.3 \times 10^{11}T_x^{1/2} \text{ s}^{-1}$.

It is worth noting that where T is smaller than T_x, superelastic collisions of H atoms and H_2 molecules with H_2O molecules add heat to the gas. In the numerical results presented in this paper, a region where $T < T_x$ occurs close to the central star.

iii) *Vibrational Excitation of* H_2O *Molecules*

The cross sections for the direct vibrational excitation of H_2O molecules by collisions with H atoms or H_2 molecules are unknown. At low energies, collisional interactions act adiabatically on the vibrational time scale. Consequently, vibrational de-excitation cross sections tend to be much smaller than elastic scattering cross sections (Rapp and Kassal 1969). Since the direct vibrational excitation rates of H_2O molecules cannot be accurately estimated, this process is not included as a source of cooling for the circumstellar gas.

A more certain mechanism for the production of vibrationally excited H_2O molecules is the exothermic reaction $H_2 + OH \rightarrow H + H_2O$. This reaction is expected to have a high probability of producing a H_2O molecule whose bending mode is vibrationally excited. The vibrationally excited H_2O molecules decay radiatively[1] and thus contribute to the cooling of the gas. This radiative loss contributes a heat loss rate per unit volume

$$C_2 \approx \frac{k^+\Delta}{2}\,n_{OH}n_{H_2}\ ,\quad (12)$$

where k^+ is the exothermic rate constant and Δ is the energy released for each OH molecule which is converted into a H_2O molecule. The factor of 1/2 in equation (12) is included as a guess at the fraction of the energy which goes into the vibrational excitation of the H_2O molecule. A discussion of the relevant rate constants for exchange reactions involving H, H_2, O, OH, and H_2O is presented in § IIc so values for k^+ and Δ are not included here. It is important to note that the cooling rate given by equation (12) represents a lower limit to the actual cooling rate due to the vibrational excitation of H_2O molecules because direct vibrational excitation has been neglected.

iv) *Vibrational Excitation of* H_2 *Molecules*

Several factors combine to make the cooling rate due to H_2 vibrational excitation easy to calculate. First, vibrational excitation by the stellar radiation is unimportant except very close to the central star and may be neglected. Second, the vibrational level spacing is large (~ 0.6 eV); thus only collisional excitation of the first excited vibrational state need be considered. Third, the rotation-vibration transitions are optically thin even in the dense inner parts of the circumstellar envelope so that radiative transfer effects are negligible.

The heat loss rate per unit volume due to the emission of $2\ \mu$ photons in rotation-vibration transitions from the first excited to the ground vibrational state is given by

$$C_3 = A_{1,0}h\nu_{1,0}n_1\ ,\quad (13)$$

where $A_1 \approx 3 \times 10^{-7} \text{ s}^{-1}$ is the spontaneous emission rate from the first excited vibrational state and $h\nu_{1,0} \approx 0.6$ eV is the energy of the emitted photon.

---

[1] Although many of the stronger rotation-vibration transitions are optically thick, their net decay rates are much larger than their collisional de-excitation rates.

The number density of vibrationally excited H_2 molecules is just

$$n_1 = n_{H_2} \left\{ \frac{(n_H \langle \sigma^* v_{th} \rangle_H + n_{H_2} \langle \sigma^* v_{th} \rangle_{H_2}) \times \exp(-h\nu_{1,0}/kT)}{(n_H \langle \sigma^* v_{th} \rangle_H + n_{H_2} \langle \sigma^* v_{th} \rangle_{H_2}) \times [1 + \exp(-h\nu_{1,0}/kT)] + A_{1,0}} \right\}, \quad (14)$$

where $\langle \sigma^* v_{th} \rangle_H$ and $\langle \sigma^* v_{th} \rangle_{H_2}$ are the de-excitation rate constants for collisions of vibrationally excited H_2 molecules with H atoms and H_2 molecules, respectively. Note that at low densities, $A_{1,0}$ is the dominant term in the denominator of equation (14), hence $n_1 \propto n_{H_2}{}^2$ (for fixed $f = n_H/n_{H_2}$), whereas at high densities, the $A_{1,0}$ term is unimportant and $n_1/n_{H_2} = [1 + \exp(h\nu_{1,0}/kT)]^{-1}$ which is the value appropriate to thermal equilibrium.

At low energies, the vibrational de-excitation cross sections are very much smaller than the elastic scattering cross sections because the collisional interactions act nearly adiabatically on the vibration time scale. Also, $\langle \sigma^* v_{th} \rangle_H \gg \langle \sigma^* v_{th} \rangle_{H_2}$ at low T because the repulsive potential energy at small separations is lower for the $H-H_2$ system than for the H_2-H_2 system.

The values of $\langle \sigma^* v_{th} \rangle_H$ used in this paper are adapted from exact quantum mechanical calculations of $H-H_2$ scattering by Schatz (1975). The theoretical values of $\langle \sigma^* v_{th} \rangle_H$ are well fit by the relation

$$\langle \sigma^* v_{th} \rangle_H = 1.64 \times 10^1 T^{-2.93}$$

$$\times \exp[-100/T^{1/3}] \quad cm^3 \, s^{-1} \quad (15)$$

for $T < 4 \times 10^3$ K. The theoretical formula is in good agreement with the single experimental measurement of $\langle \sigma^* v_{th} \rangle_H = 3 \times 10^{-13}$ cm^3 s^{-1} at $T = 299$ K by Heidner and Kasper (1972).

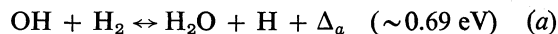For H_2-H_2 scattering, $\langle \sigma^* v_{th} \rangle_{H_2}$ is experimentally determined for 1100 K $< T < 2700$ K by Kieffer and Lutz (1966) and for a single point at $T = 300$ K by DeMartini and Ducuing (1966). All of the data are adequately represented by the relation

$$\langle \sigma^* v_{th} \rangle_{H_2} = 3.54 \times 10^{-13} T \exp[-100/T^{1/3}] \quad cm^3 \, s^{-1}.$$
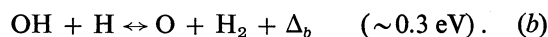$$(16)$$

The total heat loss rate C used in equation (8) is given by $C = C_1 + C_2 + C_3$.

d) Chemical Exchange Reactions

The central stars in OH–IR sources are oxygen rich, that is [O]/[C] > 1. In the circumstellar envelopes essentially all of the C atoms are expected to be bound in CO molecules. The excess O atoms are bound in OH and H_2O molecules or exist in the form of atomic O. The relative abundances of these three species are affected by the chemical exchange reactions

$$OH + H_2 \leftrightarrow H_2O + H + \Delta_a \quad (\sim 0.69 \text{ eV}) \quad (a)$$

and

$$OH + H \leftrightarrow O + H_2 + \Delta_b \quad (\sim 0.3 \text{ eV}). \quad (b)$$

These reactions have activation energies, $A_a \approx 0.3$ eV and $A_b \approx 0.26$ eV, and rate constants in the forward (exothermic) direction, $k_a{}^+ = 10^{-10}$ cm^3 s^{-1}, $k_b{}^+ = 10^{-11}$ cm^3 s^{-1} (Carroll and Salpeter 1966). Numerical calculations of the evolution of the abundances of O, OH, and H_2O in the circumstellar gas proceed from the equations

$$v \frac{dn_{H_2O}}{dr} = [n_{OH} n_{H_2} k_a{}^+ - n_{H_2O} n_H k_a{}^- \exp(-\Delta_a/kT)]$$
$$\times \exp(-A_a/kT),$$

$$v \frac{dn_O}{dr} = [n_{OH} n_H k_b{}^+ - n_O n_{H_2} k_b{}^- \exp(-\Delta_b/kT)]$$
$$\times \exp(-A_b/kT), \quad (17)$$

and

$$n_O + n_{OH} + n_{H_2O} = 10^{-3} n_{H_2}(1 + f/2).$$

In applications of equations (17), $k_a{}^- = k_a{}^+/2$ and $k_b{}^- = 2k_b{}^+$ are used. These relations are only approximate and do not accurately take into account the T dependence of the partition functions.

The rates of the exchange reactions involving O, OH, and H_2O depend upon the value of $f \equiv n_H/n_{H_2}$. In the numerical calculations reported upon in this paper $f = 1$ is always used. It is easily verified from the numerical results that only a negligible fraction of the H_2 molecules are dissociated during the ejection of circumstellar gas from the star. The appropriate dissociation rate constants for $H-H_2$ and H_2-H_2 collisions are

$$k_{H-H_2} = 8k_{H_2-H_2} = \frac{1.4 \times 10^{-4}}{T^{1.025}}$$

$$\times \exp(-55,196/T) \quad cm^3 \, s^{-1}, \quad (18)$$

where T is in kelvins. These rate constants are derived from the corresponding recombination rates which have been measured by Jacobs, Giedt, and Cohen (1967). The actual value of f should be matched to conditions at the base of the flow in the stellar atmosphere. From the appropriate rates for three-body recombinations and collisional dissociations, it is found that n_H/n_{H_2} is frozen out at a level somewhat above the stellar photosphere. Atmospheric models of late M-type giants and supergiants by Vardya (1966) show that $0.1 < f \lesssim 1$ at these levels in the atmosphere.

All of the aforementioned considerations concerning the value of f only apply if the mass outflow is driven by radiation pressure. If mass is ejected by shock waves, then significant dissociation of H_2 molecules might occur. However, the theoretically predicted OH abundance is much more sensitive to T than it is to f. Thus it would serve no purpose to consider different values of f in this investigation.

III. NUMERICAL RESULTS

The expansion velocity of the circumstellar gas is derived by integrating equation (1) with the aid of
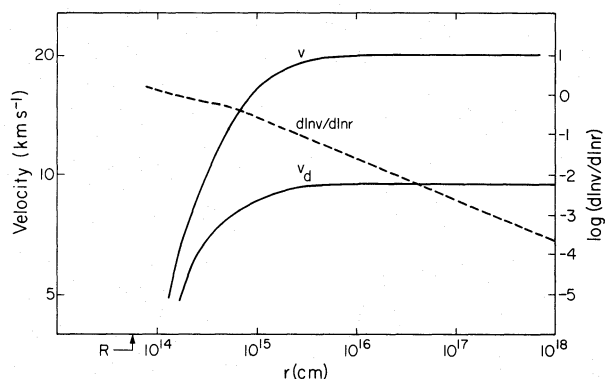
FIG. 1.—The streaming velocity of the circumstellar gas v and the relative velocity at which the dust grains move through the gas v_d are shown as a function of the radial distance r.

$\kappa(r)$ from equation (3) and the mass loss integral $\Phi = 4\Pi r^2 n_{H_2} m_{H_2}(1 + f/2)v$. This integration can be performed analytically. The behavior of $v(r)$ is illustrated in Figure 1. Once $v(r)$ is known, equations (8) and (17) are integrated simultaneously to obtain T, n_O, n_{OH}, and n_{H_2O} as functions of r. These results are displayed in Figures 2–4. The gas kinetic temperature shows a gradual decline with increasing distance from the central star. Except very close to the central star, friction between the dust and the gas is the main source of heat input. The dominant cooling mechanism close to the star is the radiation of photons by vibrationally excited H_2O molecules. Radiation losses due to pure rotational transitions of H_2O molecules are most important at intermediate distances. At large distances from the central star, the gas cools by adiabatic expansion. At all radii, n_O and n_{OH} are much smaller than n_{H_2O}. For $r \lesssim 2 \times 10^{15}$ cm, the relative abundances of O, OH, and H_2O are those appropriate to chemical equilibrium at the ambient gas temperature. For $r \gtrsim 2 \times 10^{15}$ cm, T is so low ($T < 500$ K)
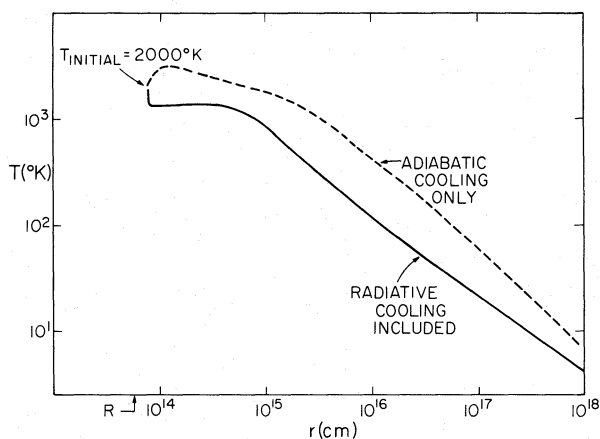

FIG. 3.—The rates of the principal contributions to the heating and cooling of the circumstellar gas are graphed as functions of the radial distance r. Note that the ordinate has a broken scale with contributions to the heating plotted in the lower half of the diagram and contributions to the cooling plotted in the upper half. Furthermore, the values of the heating and cooling rates are scaled by the factor $(r/10^{14})^4$.

FIG. 2.—The gas kinetic temperature T is plotted against the radial distance r. The solid curve is based on a calculation which includes cooling due to both radiative losses and expansion. The dashed curve is taken from a calculation which only includes cooling due to adiabatic expansion.
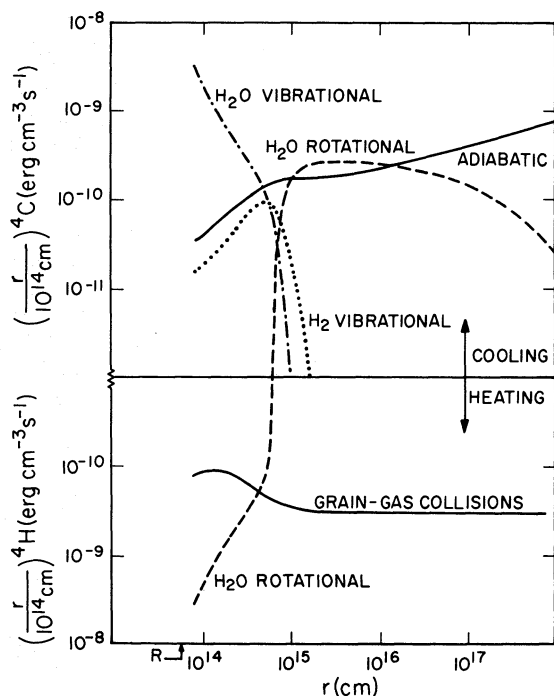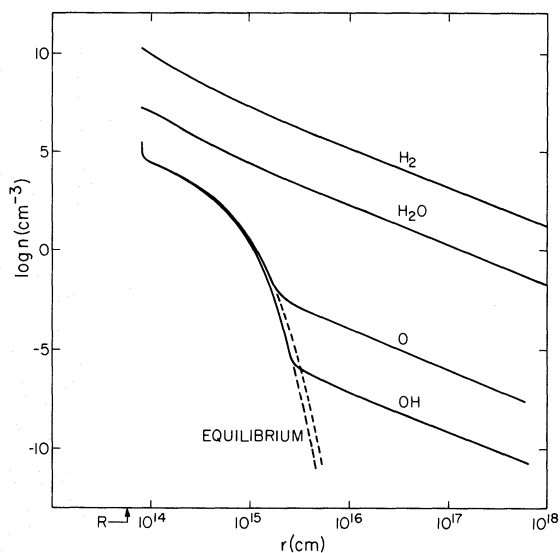

FIG. 4.—The atomic and molecular abundances are shown as a function of radial distance r. The OH and O abundances appropriate to chemical equilibrium at the ambient gas temperature are given by the dashed curves.

that the relative abundances of O, OH, and H_2O are frozen out at constant values.

It is hoped that the calculations just described provide a reliable estimate for $T(r)$ in the circumstellar envelopes of OH–IR stars. However, it must be stressed that these calculations involve several crucial assumptions and approximations. Among these, perhaps the most significant are the assumed mass loss rate $\Phi = 3 \times 10^{-5} \, M_\odot \, \text{yr}^{-1}$, the assumed form of the dust opacity $\kappa(r)$, and the rough approximation to the H_2O rotational cooling. It is important to evaluate how changes in these basic assumptions and approximations might affect the calculated behavior of $T(r)$.

The mass loss rate is not directly determined from observation. It is inferred from infrared observations which provide reasonable estimates for the dust opacity in the circumstellar envelopes. Without knowledge of the size distribution of the dust grains and the fraction of the condensable material that actually forms into grains, the deduction of a mass loss rate is rather uncertain. The value of $\Phi = 3 \times 10^{-5} \, M_\odot \, \text{yr}^{-1}$ is consistent with the infrared observations, but is not uniquely determined by them. There is also a dynamical method which may be used to determine Φ. This method assumes that L, R, M, $\kappa(r)$, and v_∞ are known. For fixed L, R, M, and $\kappa(r)$, integration of the momentum equation then yields a unique relation between v_∞ and Φ. The values of Φ obtained by this method are again of order 3×10^{-5} $M_\odot \, \text{yr}^{-1}$. The value of Φ is important because for fixed v_∞ the heat input rate per unit mass due to collisions between dust grains and gas molecules is proportional to $[Q\kappa(r)/\Phi]^{1/2}$. Since the adiabatic cooling rate per unit mass is independent of Φ and the H_2O rotational cooling rate per unit mass varies inversely with Φ, the circumstellar gas temperature is a monotonically decreasing function of Φ.

The heat input per unit mass is proportional to $\kappa(r)$. The smallest value of κ_∞ compatible with a given value of v_∞ is achieved if $\kappa(r)$ rises abruptly from zero to κ_∞ just above the stellar surface. The assumption adopted in this paper, that $\kappa(r)$ increases gradually until $r \approx 20 \, R$, results in the prediction of higher values of T at large r ($r > 20 \, R$) than would be predicted if $\kappa(r)$ attained its maximum value near the stellar surface.

The derivation of the H_2O rotational cooling rate is very crude. Better calculations are certainly possible, but definitive results are a long way off. Fortunately, in the mass loss range that seems to characterize OH–IR stars, $\Phi \approx 3 \times 10^{-5} \, M_\odot \, \text{yr}^{-1}$, adiabatic cooling is comparable with H_2O rotational cooling in the outer regions of the circumstellar envelopes where the OH masers appear to operate.

If the values of $T(r)$ that are predicted by the calculations are accepted as valid estimates, then one can draw several important conclusions concerning the predicted OH abundance in the circumstellar envelope. The predicted values of the OH abundance are very low, $n_{OH} < 1 \, \text{cm}^{-3}$ for $r > 10^{15}$ cm. These low values of n_{OH} are incompatible with very long baseline interferometry observations which show that OH masers

operate in the outer envelopes ($r \gg 10^{15}$ cm) of OH–IR stars and theoretical calculations which indicate that OH column densities of order $10^{17} \, \text{cm}^{-2}$ are the minimum values compatible with the observed brightness temperatures.[2] This suggests that an as yet unidentified mechanism must be responsible for producing OH molecules in abundances that are compatible with those implied by the observed masers. Another important point is that for $r > 2 \times 10^{15}$ cm, OH molecules are not destroyed at a significant rate, since T is so low. Thus the mechanism which produces the OH molecules that are required by the masers probably operates at $r > 10^{15}$ cm. Of course, nothing can be deduced about whether or not it operates at $r < 10^{15}$ cm.

IV. H_2O PHOTODISSOCIATION

The photodissociation of H_2O molecules by interstellar ultraviolet photons is a significant source of OH molecules in the outer envelopes of OH–IR sources. About 90 percent of the photodissociations yield OH + H and the remaining 10 percent yield O + H_2 (Carroll and Salpeter 1966). From the interstellar ultraviolet photon density (Witt and Johnson 1973) and the absorption coefficient for H_2O photodissociation (Thompson, Harteck, and Reeves 1963), the photodissociation rate in the unshielded interstellar radiation field is estimated to be roughly $10^{-9} \, \text{s}^{-1}$.

In order to calculate the abundance of OH molecules produced by the photodissociation of H_2O molecules in the circumstellar envelopes which surround OH–IR stars, it is necessary to take into account the attenuation of the interstellar ultraviolet radiation by both the H_2O molecules and the dust grains. The OH abundance is numerically calculated from the equations

$$v \frac{dn_{OH}}{dr} = n_{H_2O} \left[0.9c \int n_\lambda \sigma_{H_2O}(\lambda) d\lambda - \frac{2v}{r} \right] \quad (19)$$

and

$$\frac{1}{n_\lambda} \frac{dn_\lambda}{dr} = n_{H_2O} \sigma_{H_2O}(\lambda) + n_d \sigma_d(\lambda) , \quad (20)$$

subject to the boundary conditions that all of the oxygen which is not bound in CO is in H_2O at an inner radius of 5×10^{14} cm ($n_{H_2O}/[n_{H_2}(1 + f/2)] = 10^{-3}$ at $r = 5 \times 10^{14}$ cm). Because T is so low in the region where appreciable photodissociation occurs, the chemical reaction of OH with H_2 is not included in this calculation. Two separate calculations were performed in order to assess the importance of the shielding provided by the dust grains. One calculation uses an ultraviolet dust opacity equal to 15 times the near-infrared opacity given by equation (3), while the other calculation neglects the ultraviolet dust opacity entirely. The numerical results are displayed in Figure 5. The OH number density reaches a maximum of $n_{OH} \approx 4 \, \text{cm}^{-3}$ at $r \approx 3 \times 10^{16}$ cm. This result is only

---

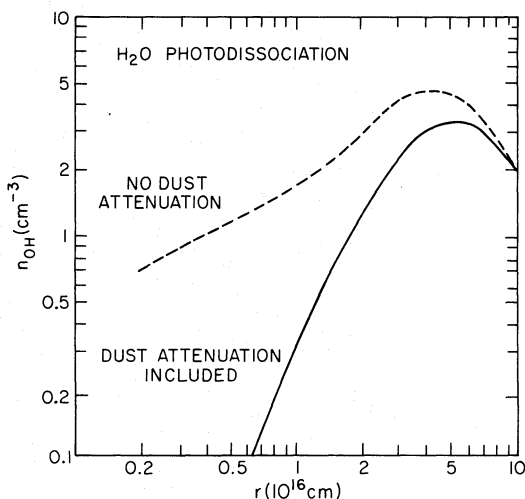[2] These points are discussed in more detail in Elitzur, Goldreich, and Scoville (1975).

Fig. 5.—The photodissociation of H_2O molecules by interstellar ultraviolet radiation is an important source of OH molecules in the outer part of the circumstellar envelope. The solid curve illustrates the OH abundance obtained from a calculation which includes the attenuation of the ultraviolet radiation by circumstellar dust. The dashed curve is taken from a calculation in which the dust attenuation is neglected.

slightly dependent upon the shielding provided by the dust grains as a comparison of the curves labeled "dust" and "no dust" shows.

The photodissociation rate of OH molecules in the interstellar ultraviolet radiation field is unknown, but it has traditionally been thought to be much lower than 10^{-9} s^{-1}. For this reason, the photodissociation of OH molecules has not been included in the calculations. Should the OH photodissociation rate turn out to be comparable with the H_2O photodissociation rate, the calculated OH abundances might be considerably too high.

The H_2O molecules are photodissociated by ultraviolet photons with $\lambda \approx 1650$ Å. These photons come primarily from O and B stars which are relatively rare and tend to be grouped in associations. Consequently, the incident ultraviolet flux is not equal at all OH–IR stars and may even vary significantly between opposite sides of the same star. Habing (1968) estimates that in 10 percent of the volume near the galactic plane, the ultraviolet radiation density may deviate from the average value by more than a factor of 3 due to the nearest OB association. It is possible that anisotropies in the ultraviolet flux are responsible for the different intensities of the two 1612 MHz emission features in some sources.

Strong shock waves driven by pulsational and convective motions in the atmospheres of the central stars could ionize a fraction of the circumstellar gas. The recombination radiation from the ionized gas might be a significant source of ultraviolet photons capable of photodissociating H_2O molecules. Sensitive studies of the radio emission from OH–IR stars would permit observational limits to be set on the amount of ionized circumstellar gas. Radio emission at $\lambda = 2.8$ cm has been detected from one OH–IR star, NML

Cygnus, by Goss, Winnberg, and Habing (1974). If, as seems most probable, this radiation arises from optically thin free-free emission, the implied rate of emission of Balmer continuum photons with 1500 Å < λ < 1800 Å is $10^{41} \exp(-8.71/T_4)$ s^{-1} ($T = 10^4 T_4$ K). This rate is to be compared with the calculated rate of H_2O photodissociation by interstellar ultraviolet which is 10^{41} s^{-1} inside $r = 3 \times 10^{16}$ cm. Thus it is possible that in NML Cygnus, the H_2O photodissociation rate due to recombination radiation is comparable with that due to interstellar ultraviolet radiation if the ionized circumstellar gas is hot ($T_4 \gtrsim 1$). However, H_2O photodissociation due to circumstellar recombination radiation would occur very close to the central star where the gas temperature is high ($T > 10^3$ K), and the OH molecules which are produced would rapidly be converted back to H_2O molecules by reaction with H_2 molecules. Thus it is doubtful whether circumstellar recombination radiation can make an important contribution to the production of the OH molecules involved in the maser emission.

V. DISSOCIATION OF H_2O MOLECULES BY COLLISIONS WITH DUST GRAINS

The velocity at which the dust grains stream through the gas is large. With the parameters appropriate to the standard model adopted in this paper, $v_d = 9$ km s^{-1}. The kinetic energy of an H_2O molecule moving with a velocity of 9 km s^{-1} is 7.7 eV which is greater than the 5.2 eV required to dissociate the H_2O molecule into an OH molecule and an H atom. This raises the possibility that OH molecules are produced by collisions between H_2O molecules and dust grains. To test the significance of this process for the production of circumstellar OH molecules, the numerical calculations described in § III were repeated with a slight change. Terms $-\sigma_d n_d v_d n_{H_2O}$ and $\sigma_d n_d v_d n_{OH}$ were added to the expressions for dn_{H_2O}/dt and dn_O/dt in equations (17). The OH abundance predicted by this calculation is shown in Figure 6. Clearly, the result is an upper bound to the OH abundance that might be produced by collisions between H_2O molecules and dust grains, since it is assumed that every collision gives rise to an OH molecule.

For the standard model circumstellar envelope, the collisional dissociation of H_2O molecules gives rise to an OH column density which is near the minimum value required for strong maser amplification.

H_2 molecules are less likely to be dissociated by collisions with dust grains than are H_2O molecules because the H_2 molecules are lighter. At 9 km s^{-1} the kinetic energy of a H_2 molecule is just 0.85 eV which is much lower than its dissociation energy of 4.48 eV.

VI. EFFECTS OF STELLAR VARIABILITY

The central stars in many OH–IR sources are Mira variables whose periods are of order 2 years. The intensities of the 1612 MHz masers associated with these stars vary in phase with the stellar luminosity (Harvey et al. 1974). The same is true of the intensities
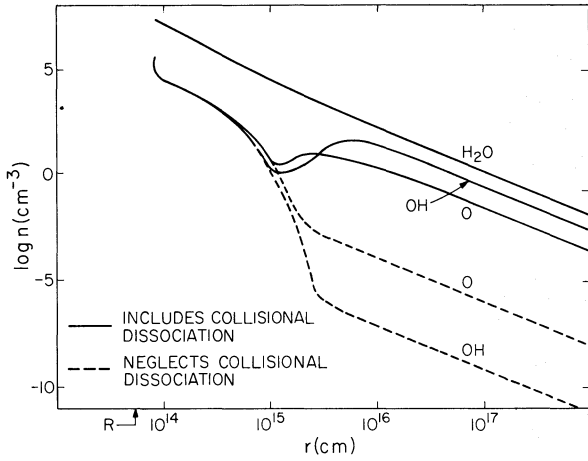
FIG. 6.—The dissociation of H_2O molecules in collisions with dust grains produces OH molecules. The predicted upper limit to the OH abundance produced by this mechanism is shown as a function of radial distance r. For reference, the H_2O and O abundances are also included.

of the 2.2 GHz H_2O masers associated with Mira variables (Schwartz, Harvey, and Barrett 1974). Since the ultimate goal of this investigation is to provide information that will aid in the understanding of the maser pump mechanisms, it is essential to study how the stellar luminosity variations affect the circumstellar gas.

The stellar luminosity variations impose variations in the velocity at which the dust grains move through the gas. The variations of v_d are governed by

$$m_d \frac{dv_d}{dt} = \frac{\sigma_d Q_d L(t)}{4\Pi r^2 c} - \sigma_d m_{H_2} n_{H_2} (1 + f/2) v_d^2 . \quad (21)$$

Although the luminosity variations of the central stars in many OH–IR sources are quite large, only the small amplitude limit is studied here. The small amplitude limit is simple and suffices to illustrate all of the essential physics. The luminosity $L(t)$ is assumed to be given by

$$L(t) = L^{(0)} + L^{(1)} = L^{(0)} + \hat{L}^{(1)} \cos \omega t , \quad (22)$$

where $\hat{L}^{(1)}/L^{(0)} \ll 1$. Since $\omega r/v \gg 1$, equation (21) may be integrated with n_{H_2} and r treated as constants. The resulting expression for v_d may be written as $v_d = v_d^{(0)} + v_d^{(1)}$, where $v_d^{(0)}$ is given by equation (10) and

$$\frac{v_d^{(1)}}{v_d^{(0)}} = \frac{\hat{L}^{(1)}}{2L^{(0)}[1 + (\omega\tau/2)^2]^{1/2}}$$

$$\times \cos [\omega t - \tan^{-1} (\omega\tau/2)] . \quad (23)$$

Here

$$\tau = \frac{m_d}{m_{H_2} n_{H_2} (1 + f/2) \sigma_d v_d^{(0)}} \quad (24)$$

is the time required for a dust grain to collide with a mass of gas equal to its own mass (Gilman 1972).

In the outer parts of the circumstellar envelope ($r > 10^{15}$ cm) the cooling time is comparable with the expansion time. Thus to a first approximation, the cooling processes may be neglected when calculating how T varies in response to the variation in v_d. The expression for $T^{(1)}$ as calculated from equation (8) is

$$T^{(1)} = \frac{\hat{L}^{(1)} m_{H_2} (1 + f/2) \sigma_d n_d (v_d^{(0)})^3}{L^{(0)} k \omega (1 + f)[1 + (\omega\tau/2)^2]^{1/2}}$$

$$\times \sin [\omega t - \tan^{-1} (\omega\tau/2)] . \quad (25)$$

For $r \gtrsim 10^{15}$ cm, the numerical evaluation of equations (24) and (25) yields

$$T^{(1)} \approx \frac{1.9 \times 10^2 \hat{L}^{(1)}}{r_{15}^2 L^{(0)}[1 + (\omega\tau/2)^2]^{1/2}}$$

$$\times \sin [\omega t - \tan^{-1} (\omega\tau/2)] \text{ K} \quad (26)$$

and

$$\omega\tau = 5.7 \times 10^{-2} r_{15}^2 , \quad (27)$$

where $r = 10^{15} r_{15}$ cm. In deriving these numerical results, the standard model parameters were used. In addition, it was assumed that $P = 2\Pi/\omega = 2$ yr, $m_d = 4\Pi a_d^3 \rho_d/3$, $a_d = 10^{-5}$ cm, $\rho_d = 3$ gm cm^{-3}. The restriction to $r \gtrsim 10^{15}$ cm arises because the variations of the cooling rates with T have been neglected and the asymptotic values for $\sigma_d n_d$, v, $v_d^{(0)}$ appropriate to large r have been used.

The important point to recognize from equations (26) and (27) is that the variation in T lags the variation in L by $\Pi/2$ radians if $\omega\tau \ll 1$ and by Π radians if $\omega\tau \gg 1$.

APPENDIX

H_2O ROTATIONAL EXCITATION

The populations of the rotational levels of the ground vibrational state of the H_2O molecule are affected by collisions, by the absorption of radiation from the central star, and by spontaneous emission. All of the essential factors which determine the excitation temperatures of the rotational transitions may be illustrated in terms of a

model molecule which has three scalar levels, two rotational levels in the ground vibrational state, and one rotational level in an excited vibrational state. Each level is connected to the other two levels by radiative transitions.[3]

The rate equations whose steady-state solutions determine the level populations are written below:

$$\frac{dn_1}{dt} = \beta_{21}A_{21}n_2 + (A_{31} + B_{31}J_{13})n_3 - B_{13}J_{13}n_1 - C[n_1 \exp(-h\nu_{21}/kT) - n_2],$$ (A1a)

$$\frac{dn_2}{dt} = \beta_{21}A_{21}n_2 + (A_{32} + B_{32}J_{23})n_3 - B_{23}J_{23}n_2 + C[n_1 \exp(-h\nu_{21}/kT) - n_2],$$ (A1b)

$$n_1 + n_2 + n_3 = n.$$ (A1c)

The notation used in equations (A1) needs some explanation. The molecular levels are labeled 1, 2, and 3 in order of increasing energy. The n_i are the populations per unit volume of each level, and n is the total molecular number density. The net radiative decay rate of level 2 is expressed as $\beta_{21}A_{21}$. Here A_{21} is the spontaneous decay rate of level 2, and β_{21} is the probability that an emitted photon will escape without further interaction. Since the streaming velocities in the circumstellar envelope are much greater than the thermal velocity of the H_2O molecules, the escape probability is locally determined and is given by (Castor 1970)

$$\beta_{21}(r) = \int_0^1 \frac{1 - \exp[-\tau_{21}(r, \mu)]}{\tau_{21}(r, \mu)} d\mu,$$ (A2)

where $\tau_{21}(r, \mu)$ is the optical depth along a ray which makes an angle $\theta = \cos^{-1}\mu$ with the radius vector at r.

$$\tau_{21}(r, \mu) = \frac{hcr}{4\Pi v} \frac{B_{12}(n_1 - n_2)}{[1 + \mu^2(d\ln v/d\ln r - 1)]}.$$ (A3)

The important H_2O rotational transitions are optically thick so that

$$\beta_{21}(r) = \frac{8\Pi v}{3hcrB_{12}(n_1 - n_2)}\left(1 + \frac{1}{2}\frac{d\ln v}{d\ln r}\right),$$ (A4)

and

$$\beta_{21}(r)A_{21} = \frac{16\Pi v}{3r\lambda_{21}{}^3(n_1 - n_2)}\left(1 + \frac{1}{2}\frac{d\ln v}{d\ln r}\right).$$ (A5)

The contribution that the stellar radiation at frequency ν_{21} makes to the transitions between levels 1 and 2 has been neglected. It could be included by adding terms equal to $\pm(T_e/T_x)\epsilon W\beta_{21}A_{21}n_2$ to equations (A1a) and (A1b), respectively. Here W is the dilution factor for the stellar radiation at r,

$$W = \frac{1}{2}\left\{1 - \left[1 - \left(\frac{R}{r}\right)^2\right]^{1/2}\right\} \approx \frac{1}{4}\left(\frac{R}{r}\right)^2$$ (A6)

for $R/r \ll 1$ and

$$\epsilon = \frac{d\ln v}{d\ln r}.$$ (A7)

Except very close to the central star, $(T_e/T_x)W\epsilon \ll 1$ so that the transition rate between levels 1 and 2 due to the stellar radiation is small compared with the net radiative decay rate of level 2.

Population is indirectly transferred between levels 1 and 2 by transitions that involve level 3. Radiative transitions between levels 1 and 3 and between levels 2 and 3 are included in equations (A1). Collisional transitions between the ground and excited vibrational states are neglected because their rates are much slower than the radiative rates. The relative slowness of the collisional rates is in part due to vibrational adiabaticity which makes the collisional cross sections for vibrational de-excitation much smaller than the geometrical cross sections at low energies. The radiative rates between levels 1 and 3 and between levels 2 and 3 depend upon the intensity in these lines averaged over the line profile. As shown by Castor (1970), the profile averaged mean intensity for an optically thick line is given by

$$J_{ij}(r) = \epsilon WB_{\nu_{ij}}(T_e),$$ (A8)

where $B_{\nu_{ij}}(T_e)$ is the Planck function.[4]

[3] The radiative linkage assumed for the model molecule is not realized in actual molecules, since electric dipole transitions only occur between levels of opposite parity. However, the effects of the more complicated radiative linkages, involving more than three levels, that occur in the H_2O molecule are well simulated by this simple model.

[4] As will be verified later, the strong rotation-vibration lines which arise from the ground vibrational state of the H_2O molecule are optically thick in the circumstellar envelopes. However, their optical depths are not very large. If the lines were optically thin, then $J_{ij} = WB_{\nu_{ij}}(T_e)$ would be the appropriate expression for the profile averaged mean intensity.

The last terms on the right-hand sides of equations (A1a) and (A1b) describe the collisional transfer of population between levels 1 and 2. In all numerical applications, the collisional rate C is set equal to

$$C = 2 \times 10^{-11} T^{1/2} n_{\mathrm{H_2}} (1 + f) \quad \mathrm{s}^{-1}. \tag{A9}$$

With a given set of input parameters for n, v, ϵ, r, R, T, T_e, A_{ij}, v_{ij}, and C, equations (A1)–(A9) determine the steady-state level populations, n_i. If the excitation temperature of the transition between levels 1 and 2 so obtained is to approximate the excitation temperatures of the rotational transitions of the circumstellar H_2O molecules, then the values of v_{ij} and n must be chosen with some care. Appropriate values for these quantities are estimated by treating the molecular rotation classically and assuming that all of the H_2O rotational transitions have the same excitation temperature T_x. The classical approximation should be an adequate one for $T_x \gtrsim 150$ K. In this limit, the rotational partition function is

$$Z_{\mathrm{rot}} = \frac{(2kT_x)^{3/2}(\Pi I_1 I_2 I_3)^{1/2}}{2h^3} ; \tag{A10}$$

the rms value of the angular velocity is

$$\Omega = \left[kT_x \left(\frac{1}{I_1} + \frac{1}{I_2} + \frac{1}{I_3} \right) \right]^{1/2} ; \tag{A11}$$

and the rms value of the angular momentum is

$$M = [kT_x(I_1 + I_2 + I_3)]^{1/2} \tag{A12}$$

(Landau and Lifshitz 1958). The molecular moments of inertia for the H_2O molecule are $I_1 = 6.4 \times 10^{-40}$ gm cm², $I_2 = 1.2 \times 10^{-39}$ gm cm², and $I_3 = 1.76 \times 10^{-39}$ gm cm² (Townes and Schawlow 1955) from which it follows that

$$Z_{\mathrm{rot}} = 8.1 \times 10^{-3} T_x^{3/2}, \qquad v = \Omega/2\Pi = 1.3 \times 10^{11} T_x^{1/2} \quad \mathrm{s}^{-1}, \qquad J = M/h = 2.7 \times 10^{-1} T_x^{1/2}, \tag{A13}$$

where T_x is expressed in kelvins. The appropriate value of n to use in equations (A1)–(A9) is

$$n = \frac{2(2J + 1)}{Z_{\mathrm{rot}}} n_{\mathrm{H_2O}} \approx \frac{4J}{Z_{\mathrm{rot}}} n_{\mathrm{H_2O}} . \tag{A14}$$

The frequency v_{21} is set equal to the rms rotational frequency of the H_2O molecule. The values of v_{31}, v_{21}, A_{31}, A_{32} are taken to be characteristic of those for strong transitions in the v_3 band at $\lambda = 2.66$ μ, namely, $v_{31} = 1.13 \times 10^{14}$ Hz, $v_{32} = v_{31} - v_{21}$, and $A_{31} = A_{32} = 34$ s⁻¹. This completes the formal description of the equations and parameter values used to derive T_x. In the following paragraph, a simplified expression for H_2O rotational cooling is developed as an aid to interpreting the results which are obtained numerically from the complete set of equations (A1)–(A14).

Equations (A1a) and (A1b) may be manipulated to yield

$$C \frac{hv_{21}}{k} \left(\frac{1}{T_x} - \frac{1}{T} \right) = \beta_{21} A_{21} + \epsilon W A_{31} \left(\frac{hv_{21}}{k} \right) \exp \left(\frac{-hv_{31}}{kT_e} \right) \left(\frac{1}{T_e} - \frac{1}{T_x} \right) . \tag{A15}$$

In deriving equation (A15), several nonessential simplifying approximations have been made. They are the following: $A_{31} = A_{32}$, $\epsilon W \ll 1$, $hv_{21}/kT_x \ll 1$, $hv_{21}/kT_e \ll 1$, $hv_{21}/kT \ll 1$, and $\exp(hv_{31}/kT_e) \gg 1$. The interpretation of equation (A15) is straightforward. Collisions tend to make $T_x = T$ whereas the absorption of near-infrared photons in the v_3 band tends to make $T_x = T_e$.[5] The spontaneous emission of photons which escape into cold interstellar space, as represented by the term $\beta_{21} A_{21}$, tends to make $T_x = 0$ K. Numerical evaluation of the three terms in equation (A15) with parameter values appropriate to the standard model described in § II yields

$$\left(\frac{R}{r} \right)^2 (TT_x)^{1/2} \left(\frac{1}{T_x} - \frac{1}{T} \right) = 1.3 \times 10^{-14} \left(\frac{r}{R} \right) T_x^3 + 6 T_x^{1/2} \left(\frac{R}{r} \right)^2 \epsilon \left(\frac{1}{T_e} - \frac{1}{T_x} \right) . \tag{A16}$$

In deriving the equations for T_x, it was assumed that both the pure rotation transitions and the rotation-vibration transitions are optically thick. The validity of these assumptions is now to be checked.

The value of $\beta_{21} A_{21}$ is given by the second term on the right-hand side of equation (A16). In order to obtain the value of β_{21}, it is necessary to first calculate A_{21}. This can be done most easily by using the classical expression

---

[5] The latter conclusion is only true if $\exp(hv_{31}/kT_e) \gg 1$. Otherwise, radiative effects tend to make $T_x < T_e$ for $\epsilon W < 1$.

for the power radiated by a rotating electric dipole. The classical expression for the relevant Einstein A coefficient is readily shown to be

$$A_{21} = \frac{32\Pi^4}{3hc^3} \mu_\perp^2 \nu_{21}^3 , \tag{A17}$$

where $\mu_\perp$ is the component of the molecular dipole moment which is perpendicular to the rotation axis. The electric dipole moment of the H_2O molecule is $\mu \doteq 1.94$ debye. From $\mu_\perp = \mu \cos \phi$ and the expression for ν_{21} given by equations (A13), the spontaneous emission rate becomes

$$A_{21} = 4.8 \times 10^{-5} T_x^{3/2} \cos^2 \phi \text{ s}^{-1} , \tag{A18}$$

where T_x is in kelvins. Dividing this expression for A_{21} into the expression for $\beta_{21} A_{21}$ given in equation (A16) yields

$$\beta_{21} = 2.8 \times 10^{-10} \left(\frac{r}{R}\right) T_x^{3/2} \sec^2 \phi . \tag{A19}$$

The numerical values of $\beta_{21}(r)$ obtained from equation (A19) and Figure 2 are the following: $\beta_{21}(10^{14} \text{ cm}) = 2.6 \times 10^{-5} \sec^2 \phi$, $\beta_{21}(10^{15} \text{ cm}) = 1.1 \times 10^{-4} \sec^2 \phi$, $\beta_{21}(10^{16} \text{ cm}) = 6.1 \times 10^{-5} \sec^2 \phi$. These values demonstrate that the rotational transitions are optically thick.

The calculation of $\beta_{31} A_{31}$ proceeds from equations (A4) and (A14) which together imply

$$\beta_{31} A_{31} = \frac{4\Pi v Z_{\text{rot}}}{3r \lambda_{31}^3 n_{H_2O} J} , \tag{A20}$$

where $\epsilon \ll 1$ has been assumed and the population in the excited vibrational level has been neglected. Substitution of $v = 20$ km s^{-1}, $\lambda_{31} = 2.66$ μ, $n_{H_2O} \approx 2.6 \times 10^{34} r^{-2}$, and the expressions for Z_{rot} and J from equations (A13) into equation (A20) yields

$$\beta_{31}(r) A_{31} \approx 5.3 \times 10^{-19} T_x r . \tag{A21}$$

The values of $\beta_{21}(r)$ are obtained from equation (A21) and Figure 2 using $A_{31} = 34$ s^{-1} for the ν_3 band. These values are the following: $\beta_{31}(10^{14} \text{ cm}) = 3.1 \times 10^{-3}$, $\beta_{31}(10^{15} \text{ cm}) = 3.1 \times 10^{-2}$, $\beta_{31}(r = 10^{16} \text{ cm}) = 1.9 \times 10^{-2}$. Thus the rotation vibration lines are optically thick, but not as thick as the pure rotation lines.

REFERENCES

Carroll, T. O., and Salpeter, E. E. 1966, *Ap. J.*, **143**, 609.
Castor, J. I. 1970, *M.N.R.A.S.*, **149**, 111.
DeMartini, F., and Ducuing, J. 1966, *Phys. Rev. Letters*, **17**, 117.
Elitzur, M., Goldreich, P., and Scoville, N. 1975, to be published.
Gilman, R. C. 1972, *Ap. J.*, **178**, 423.
Goss, W. M., Winnberg, A., and Habing, H. J. 1974, *Astr. and Ap.*, **30**, 349.
Habing, H. J. 1968, *Bull. Astr. Inst. Netherlands*, **19**, 421.
Harvey, P. M., Bechis, K. T., Wilson, W. J., and Ball, J. A. 1974, *Ap. J. Suppl.*, No. 248, **27**, 331.
Heidner, R. F., III, and Kasper, J. V. V. 1972, *Chem. Phys. Letters*, **15**, 179.
Jacobs, T. A., Giedt, R. R., and Cohen, N. 1967, *J. Chem. Phys.*, **47**, 54.
Kieffer, J. H., and Lutz, R. W. 1966, *J. Chem. Phys.*, **44**, 668.

Kwok, S. 1975, *Ap. J.*, **198**, 583.
Landau, L. D., and Lifshitz, E. M. 1958, *Statistical Physics* (Reading: Addison-Wesley).
Rapp, D., and Kassal, T. 1969, *Chem. Rev.*, **69**, 61.
Salpeter, E. E. 1974, *Ap. J.*, **193**, 585.
Schatz, G. 1975, to be published.
Schwartz, P. R., Harvey, P. M., and Barrett, A. H. 1974, *Ap. J.*, **187**, 491.
Thompson, B. A., Harteck, P., and Reeves, R. R., Jr. 1963, *J. Geophys. Res.*, **68**, 6431.
Townes, C. H., and Schawlow, A. 1955, *Microwave Spectroscopy* (New York: McGraw-Hill).
Vardya, M. S. 1966, *M.N.R.A.S.*, **134**, 347.
Wickramasinghe, N. C. 1972, *M.N.R.A.S.*, **159**, 269.
Witt, A. N., and Johnson, M. W. 1973, *Ap. J.*, **181**, 363.
Zappala, R. R., Becklin, E. E., Matthews, K., and Neugebauer, G. 1974, *Ap. J.*, **192**, 109.

PETER GOLDREICH: Division of Geological and Planetary Sciences, California Institute of Technology, Pasadena, CA   91125

NICK SCOVILLE: Astronomy Department, University of Massachusetts, Amherst, MA   01002